JOURNAL OF MATERIALS SCIENCE 6 (1971) 490–508

Molecular Model of Drawing Polyethylene and Polypropylene

A. PETERLIN
Camille Dreyfus Laboratory, Research Triangle Institute, P.O. Box 12194, Research Triangle Park, North Carolina, USA

Morphological studies of plastic deformation of single crystals, thin layers, and bulk samples together with mechanical, X-ray and infra-red data revealed the existence of three stages in cold drawing of crystalline polymer: the plastic deformation of the original spherulitic structure, the discontinuous transformation of the spherulitic into fibre structure by micronecking, and the plastic deformation of the fibre structure. The initial material, which has low strength and high ductility, consist of stacks of parallel lamellae with few interlamella links. It deforms plastically by stack rotation, sliding of lamellae, phase change and twinning of crystal lattice, chain slip and tilt until the predeformed lamellae reach the position of maximum compliance for fracture by micronecking. The micronecks transform every single lamella into microfibrils of between one and three hundred angstroms in width, consisting of folded chain blocks broken off the lamella primarily by chain slip in the boundary layers between adjacent mosaic blocks. The chains bridging the crack are partially unfolded during the micronecking process. They connect in axial direction the blocks in the microfibril as intrafibrillar tie molecules. The number of microfibrils per cm of crack length increases with molecular weight. The draw ratio of the microfibrils and the axial separation in the microfibril of the originally adjacent crystal blocks increase with the average distance between microfibrils and, hence, decrease with increasing molecular weight. The concentration of micronecks in every stack of lamellae in a thin destruction zone produces a bundle of microfibrils of rather uniform draw ratio. Such a fibril measuring a few thousand angstroms in width includes the interlamella ties of the original sample as interfibrillar tie molecules connecting adjacent microfibrils. The concentration of micronecks also provides the conditions for a nearly adiabatic heating of the generated fibril by the transformation work in the destruction zone. The local temperature rise imparts so much mobility to the chains in the crystal blocks that during subsequent cooling to ambient temperature, the long period becomes adjusted to this temperature. The more or less random distribution of destruction zones in the neck makes the transformation from spherulitic to fibre structure appear to be a gradual process in spite of the discontinuous transformation in the micronecks. The plastic deformation of the new fibre structure can proceed only by longitudinal sliding of microfibrils past each other, a process limited by interfibrillar tie molecules. Hence, high molecular weight samples with many interlamella links exhibit a smaller draw ratio than lower molecular weight material. The three stages are to some extent intermixed in the neck. In the initial neck characterised by a low draw ratio and rather gentle constriction, the transformation into the fibre structure is not complete, so that some of the remains of the original microspherulitic structure are still present in the necked portion. They are destroyed during subsequent drawing which completes the transformation and also deforms the fibre structure. The sharply constricted mature neck, however, yields a high draw ratio which is composed of the draw ratio of microfibrils and of subsequent sliding motion of the microfibrils. The technically important natural draw ratio is the maximum draw ratio obtained with the sample under the conditions of the experiment. It seems to be higher than the draw ratio of the microfibrils.

1. Introduction

In the last ten years a large amount of morphological data on drawing of crystalline polymers has been collected. A good survey of the field may be found in [1-11]. The morphological, and particularly the orientational aspects, of the initial microspherulitic structure, the intermediate structure in the neck, and the final fibre structure of both polyethylene (PE) and polypropylene (PP) have been investigated by electron microscopy, wide- and small-angle X-ray scattering, light scattering, birefringence, infra-red absorption, and dichroism as a function of draw ratio and rate, temperature, mechanical, and thermal history. Special attention has been given to the first stages of deformation, i.e. to the reversible visco-elastic region and the incipient irreversible plastic deformation with the maximum stress at the yield point. The complete time, temperature, and orientation dependence of the elastic, plastic, and optical properties of the undrawn and drawn material at small constant and oscillating deformation has been thoroughly interpreted in terms of contributions of the amorphous and crystalline component [4-6, 11]. Most of the methods, such as mechanical measurements, and light and X-ray investigations, however, are handicapped by the fact that they always measure averages over the whole sample and that the observations do not sufficiently narrow the choice of morphological model. Hence, one needs additional information on the submicroscopical level, i.e. on the reaction and role of folded chain crystals, chain folds, free chain ends, and tie molecules during the deformation.

Electron microscopy of bulk samples, extremely thin membranes, and single crystals has definitely proved that the basic mechanism of plastic deformation contains, as the most important step, a discontinuous transformation from the unoriented original into the highly oriented fibre structure [3, 7-9]. Every folded chain lamella cracks and by a great many micronecks at the crack transforms into a bundle of microfibrils. The micronecking occurs in the macroscopic neck which propagates in the direction of draw through the strained bulk sample and transforms the original very ductile, and more or less spherulitic sample, into fibrous material of high tensile strength. The microfibrils contain completely oriented folded chain crystalline blocks alternating with amorphous layers in axial direction.

The information about the structural elements obtained through electron microscopy, together with the information obtained from the rest of the above mentioned methods, permitted the development of a molecular model of plastic deformation that gives a satisfactory explanation for the observed effects. The theoretical model will be presented as it can be developed on the basis of the observations made by using different physical methods. However, new experimental data is still needed to clarify a great many details – for instance on the effects of molecular weight and polydispersity – before they can be fully understood. Therefore, the model presented must not be considered as a complete and final version. It certainly will have to be modified as new data become available. In particular, it will have to be made more quantitative.

Most of the data used was collected on polyethylene (PE) and isotactic polypropylene (PP). The results are very similar to those obtained on polyoxymethylene (POM) [12, 13]. The main features of plastic deformation of crystalline polymers – particularly the process of micronecking – are so similar in all cases that the model developed for PE and thoroughly checked for PP can probably be applied to all crystalline polymers if their specific properties are properly taken into account, for instance, crystal polymorphism and hydrogen bonding. Some more radical modification is expected in the case of the nearly amorphous polymers, such as polyethylene terephthalate, or natural rubber which crystallise upon deformation.

In the drawing process one of the most important parameters is temperature. Since the deformational work in the neck is nearly completely converted to heat, the temperature of the sample increases in the neck [14]. Consequently, the drawing occurs at a higher temperature than that of the environment, which is supposed to be the temperature of drawing. The extreme case, with no heat conduction to the environment, occurs at very fast drawing (adiabatic drawing). This type of heating becomes unmeasurably small at a small strain rate because the heat generated at a low rate is dissipated so quickly to the environment (isothermal drawing). Such a situation is assumed in the experiments and explanations treated in this paper. This is no serious limitation because most of the effects caused by the temperature increase in the neck can be, at least in principle, easily derived from the temperature dependence of isothermal drawing. The tempera-

ture of the environment, i.e. the nominal temperature of drawing is substituted with the higher temperature which is reached as a consequence of the heat caused by the work of drawing (true temperature of drawing).

The preneck stage of plastic deformation was so thoroughly investigated – primarily by Stein and his co-workers [5, 11] – that it need not be treated here again. Therefore, this paper will concentrate on (1) the discontinuous transition from the spherulitic to the fibre structure and (2) the plastic deformation of the fibre structure. These two stages comprise, then, the destruction of the lamellae by micronecks, the formation of microfibrils, their incorporation in the fibre, and the deformation of the fibre structure by longitudinal sliding motion of microfibrils.

The structure of the unoriented initial material may be called either *spherulitic* or *microspherulitic* if one wishes to stress the fact that in a quenched sample one does not see fully developed spherulites but mostly the embryonic stages of spherulites, i.e. stacks of densely packed parallel lamellae. The stacks are randomly oriented as a consequence of random orientation of the great many primary nuclei produced by quenching. If the number of nuclei per unit volume is smaller, as is the case in isothermal crystallisation close to the melting point, or in crystallisation during slow cooling, the stacks can continue to grow and develop into spherulites by noncrystallographic branching of lamellae. Again in such a sample with fully grown spherulites the lamellae at every spot are stacked similarly to those in the embryonic stacks. The difference between the two cases is the correlation length of lamella orientation which is large in fully developed but small in independent embryonic spherulites, being in both cases of the same order of magnitude as the diameter of the structural unit originating from a single nucleus.

Hence, the basic element of the spherulitic structure is the folded chain lamellae packed into the many layer stacks and interconnected by a few tie molecules (fig. 1). The ties are formed by those molecules which during solidification were partially included in the crystal lattices of two different lamellae so that the intervening section connecting the lamellae was prevented from crystallisation. Their number increases with molecular weight and rate of crystallisation [17]. The thickness of the lamellae is between one and a few hundred angstroms; the lateral dimensions may be on the order of some ten thousand

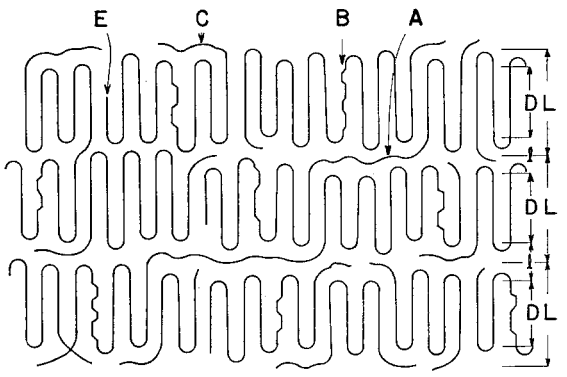

Figure 1 Stack of densely packed parallel lamellae of the microspherulitic structure (model of the starting material): A, interlamellae tie molecule, B, boundary layer between two mosaic blocks, C, chain end in the "amorphous" surface layer (cilia); E, linear vacancy caused by the chain end in the crystal lattice.

angstroms. The cohesive forces are strong within the lamellae and weak between them since they are based on Van der Waals forces between crystalline and amorphous chain conformations, respectively.

Such a structure with some modifications may be also found in as-spun fibres. The crystallisation from melt or solution in the jet between the spinnerette and the first godet results from a partially oriented medium. The orientation is caused to a minor degree by the high shear flow through the short capillary of the spinneret, but primarily by the elongational flow in the jet. The latter type of flow causes the randomly coiled macromolecules to become partially extended and oriented thus providing the material for oriented row nucleation [15]. Such linear nuclei, containing partially extended chains and oriented in the fibre axis, act as secondary nuclei for lamella growth perpendicular to the fibre axis. This epitaxial overgrowth yields cylindrical spherulites with the *b*-axis perpendicular to the row nucleus (in the case of PE). The fibres as spun seldom show such extreme orientation. Very often they are nearly isotropic or contain a mixture of cylindrical and conventional spherulites. PE and PP fibres as-spun, however, exhibit a high degree of lamella orientation perpendicular to the fibre axis and a chain orientation at a finite angle to the fibre axis [16]. In any case the parallel lamellae are packed into stacks which may have a larger extension in the fibre axis than one would expect in an isotropic spherulitic

sample. The partial orientation and extension of molecular chains before crystallisation and the ensuing row nucleation create more "tie" molecules in amorphous and crystalline conformations connecting the lamellae of the same stack than one finds in solidification from unstrained melt. But there is no evidence for the existence of a large population of microfibrils, i.e. of precursors of the fibre structure. In spite of the larger number of ties between adjacent lamellae and in the row nucleus, the structure still exhibits the basic features of the microspherulitic structure, i.e. more or less independent stacks of parallel lamellae, although their orientation, as a rule, is not more completely at random.

The final fibre structure is characterised by the nearly perfect orientation of the crystallised chains in the fibre axis, of crystal lamellae perpendicular or at a finite angle to it, and by a high longitudinal elastic modulus and tensile strength. Electron microscopy reveals the existence of microfibrils as the main element of the structure. Highly aligned in the fibre direction, they have lateral dimensions of a few hundred angstroms and a length of tens of microns. The microfibril contains folded chain crystal blocks alternating regularly with less crystalline "amorphous" regions. A great many tie molecules connect the blocks in the axial direction and impart to the microfibril a high longitudinal strength. The lateral auto-adhesion between the adjacent microfibrils is weaker since it is mainly based on van der Waals forces in the boundary layer with high crystal defect concentration (fig. 2).

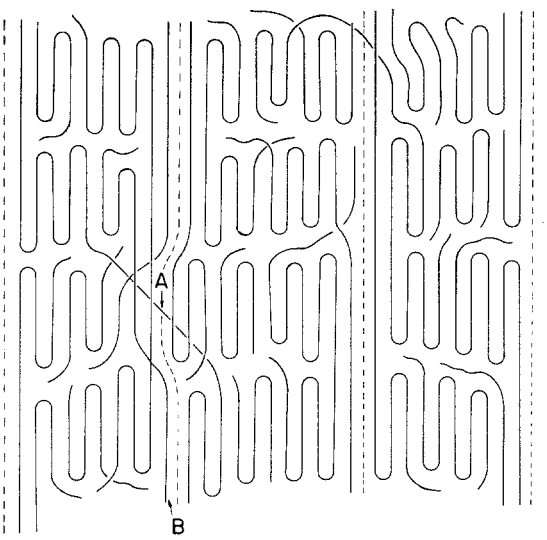

Figure 2 Microfibrillar model of the fibre structure: A, interfibrillar, B, intrafibrillar tie molecule.

2. Mechanical Aspects of Drawing

If an unoriented PE film of cross section A_0 is stretched at a constant rate, e.g. in an Instron Tensile Testing machine, a highly oriented fibrous material is obtained which finally breaks with a more or less irregular crack. The nominal stress-strain (σ_n, ϵ_n) or load-elongation (F, l_n) or (F, $\lambda_n = 1 + \epsilon_n$) curve exhibits first a linear (Hookian) region which, after a less-than-linear section, ends with a maximum, the *yield point*, characterised by a nominal yield stress $\sigma_{yn} = F_y/A_0$ and strain ϵ_{yn}. Concurrently at some weak spot a flat constriction appears which soon develops into two necks propagating through the sample in opposite directions and transforming the original film into a much stronger material (strain hardening). During this propagation the nominal *drawing stress* $\sigma_{dn} = F_d/A_0$ remains very nearly constant or increases slightly in approaching the final break characterised by the load F_b or nominal stress to break $\sigma_{nb} = F_b/A_0$. The ratio of cross sections of the original (A_0) to the transformed film (A_∞) at the time of the break yields the *natural draw ratio* $\lambda_\infty = A_0/A$, an important property of the material. It is usually derived from the length ratio of sample at break and before deformation, $\lambda_\infty = l_b/l_0$. The product $\lambda_\infty \cdot \sigma_{bn} = F_b/A_\infty = \sigma_b$ yields the true *tensile strength* (stress to break) of the drawn film. It increases almost linearly with the draw ratio [18]. With increasing molecular weight the draw ratio and stress to break decrease [18-20].

The mechanical parameters derived from the load-elongation curve are certainly rather useful for technical characterisation of a polymer sample. However, they do not reveal very much about the actual deformational response of the material and are therefore of little value for studying the deformational mechanism and its connection with the morphology of the sample. Instead, the true stress-strain curve for every volume element of the sample must be determined [14, 21]. Fig. 3 shows the true strain ϵ or $\lambda = 1 + \epsilon$ as a function of time t or nominal strain $\epsilon_n(t) = \dot{\epsilon}_n t$ for different volume elements of the PE sample. While the element still has the original microspherulitic morphology, there is first a relatively rapid elongation to a small finite

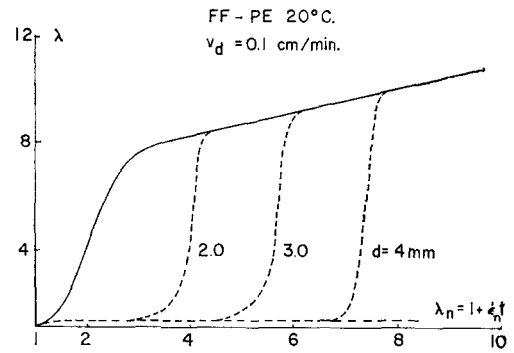

Figure 3 The true strain $\epsilon = \lambda - 1$ as function of nominal strain ϵ_n or $t = \epsilon_n/\dot{\epsilon}_n$ for volume elements with a distance 2, 3, 4 mm from the point where necking started. Quenched linear PE (Fortiflex, $M_n = 6000$, $M_w = 80{,}000$), $T_d = 20°C$, draw rate 0.1 cm/min (Meinel and Peterlin [21]).

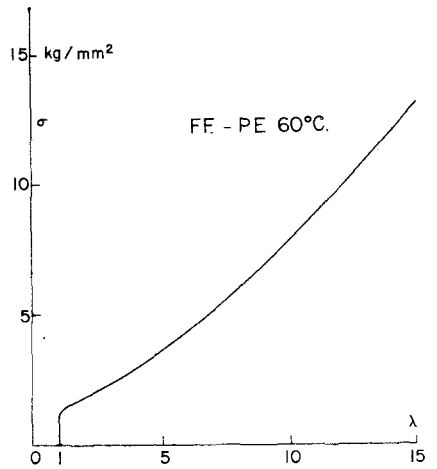

Figure 4 True stress strain curve of quenched linear PE (Fortiflex, drawn at 60° C) for the volume element where the neck started (Meinel and Peterlin [21]).

strain corresponding to the drawing stress. This strain does not change up to the moment that the neck passes through the element. The strain rate and the strain in the neck are minimum in the volume element where the neck started, and increase steadily with increasing distance of the volume element from that point, i.e. with increasing time elapsed after the original neck formation. This increase seems to be closely related to the gradually increasing sharpness of the neck. The strain continues to increase at a smaller rate even after the neck has passed over the element up to the final fracture of the sample. Three stages of plastic deformation can easily be deduced: (1) the preneck deformation of the microspherulitic structure which proceeds in the whole sample to roughly the same relatively small strain, (2) the large deformation in the neck which transforms the microspherulitic into fibre structure, and (3) the after neck deformation of the fibre structure.

The true stress-strain curve is obtained by plotting $\sigma = \lambda\sigma_n = (1 + \epsilon)\sigma_n$ over ϵ or $\lambda = 1 + \epsilon$ (fig. 4). The curves for elements at different distances from the point where the neck started are not identical, but the differences are not important for the scope of this paper. Any such curve clearly shows the steep initial Hookian region with nearly abrupt softening at the yield point where the plastic flow starts in the neck. From here on, however, the dominant feature is the gradual strain hardening as exemplified in the increase of the differential plastic modulus $d\sigma/d\epsilon$ continuing during the whole drawing process up to the final break. The two regions corresponding to the neck and to the fibre structure can be easily distinguished. In the neck the sample softens drastically for a short while as measured by the decrease of the plastic modulus. But the softening soon stops, after which the plastic modulus begins to grow as the neck passes the volume element and the morphology changes into that of the fibre structure. Such a behaviour indicates the presence of two distinct mechanisms, one (strain softening) operating in the region before the neck which prepares the microspherulitic structure for the transformation into the fibre structure, and the other (strain hardening) corresponding to the increasing fraction of the fibre structure generated in the neck.

From such a plot it is evident that the natural draw ratio is not a property established from the early beginning of the drawing process in the neck. In the experiment described in figs. 3 and 4, it is indeed the limiting draw ratio obtained after the neck has travelled over the whole length of the sample. For all but the last deformed volume element, the natural draw ratio is the sum of the drawing in the neck and the deformation of the already necked structure. The former contribution increases, the latter decreases with time. A higher gauge sample may eventually reach a limiting deformation ratio in the neck, with no detectable subsequent deformation of the fibre structure. Such a stationary state would yield the natural draw ratio immediately in the neck.

In commercial fibre drawing a steady state of fibre deformation with a natural draw ratio

(eventually, depending on the rate of drawing) is established by the constant velocity ratio of incoming as-spun fibre (v_1) and drawn fibre (v_2) $\lambda_\infty = v_2/v_1$. Every volume element is exposed to the load for the same time before it reaches the neck and the same applies to the necked (drawn) fibre. This means that in figs. 3 or 4 such fibre drawing is represented by a single curve corresponding to one fixed value of $t_1 = s_1/v_1$ between the start of the load and the passage through the neck, and similarly for the time $t_2 = s_2/v_2$ between the neck and the end of load application to the necked structure (fig. 5). From fig. 3 it can be concluded that in such a case the natural draw ratio is the sum of all three contributions although that of the neck is the most important.

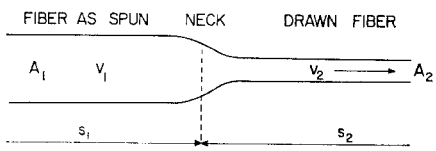

Figure 5 Velocity v, cross-section A and stress σ in the steady state fibre drawing with stationary neck shape. The distances s_1 from the feeding godet to the neck, and s_2, from the neck to the collecting godet, remain constant.

The true differential plastic modulus $d\sigma/d\epsilon$ is very large at $\lambda = 1$, but quite rapidly reaches the minimum as the neck develops. After the neck it increases with a gradually smaller slope (fig. 6). The stress to break (σ_b) and the elastic modulus $E = (d\sigma/d\epsilon)_{\epsilon=0}$, both measured at $-180°C$ in order to avoid plastic deformation, increase very nearly linearly with λ. For a PE sample drawn at 60°C, they reach saturation values in the draw ratio range between 15 and 20. All three properties plotted in fig. 6 very clearly demonstrate the strain hardening of the sample, which resists elastic and plastic deformation and fracture as a consequence of the increasing contribution of the new fibre structure generated in the neck and also, at least in the volume elements close to the starting neck, in the already necked portion of the sample.

Up to $\lambda = 8$ the effects seem to be very nearly independent of the temperature of drawing [22]. At a higher draw ratio, however, the strain hardening is much less conspicuous and reaches earlier saturation values if the drawing is performed at higher temperature [21]. A similar

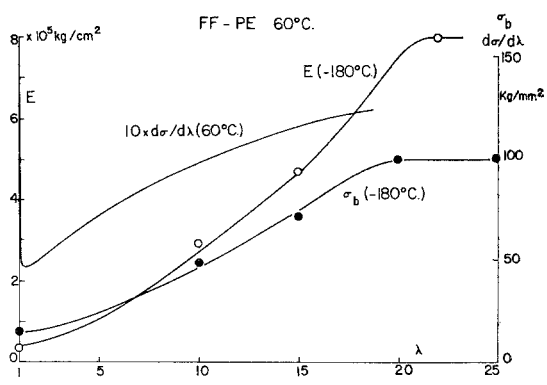

Figure 6 Elastic modulus $E = (d\sigma/d\epsilon)_{\epsilon=0}$, stress to break σ_b of quenched linear PE (see fig. 4) both measured at $-180°C$, and the differential plastic modulus $d\sigma/d\epsilon$, measured at 60°C, as functions of draw ratio λ.

conclusion about the temperature effect can be derived from the effect of annealing on the elastic modulus: it drops slowly up to $T_A = 120°C$, but above this temperature of annealing it drops very rapidly to a value not much above that of the undrawn PE [23].

Additional information about the plastic deformation can be obtained from the consideration of the differential work density [21]

$$dW/d\lambda = \sigma/\lambda = \sigma_n$$

plotted as function of λ of the volume element under consideration (fig. 7). It shows – more clearly than the load-elongation curve – the deformational mechanisms: the plastic and elastic deformation before the neck, the transformation in the neck, and the plastic deformation of the fibre structure. Moreover, it allows a simple calculation of the deformation work density

$$W = \int_1^\lambda (\sigma/\lambda)\, d\lambda = \int_1^\lambda \sigma_n\, d\lambda$$

and using simple assumptions about the transformation of morphology in the neck, a separation of the contributions of all three formerly mentioned mechanisms ($W = W_1 + W_2 + W_3$). The second term W_2 gives the work density for transformation of microspherulitic into fibre structure. The first term W_1 is very small because of the small strain the sample experiences in the unnecked portion.

The investigation of mechanical aspects of plastic deformation during the tensile experiment is the basis for the technical application of

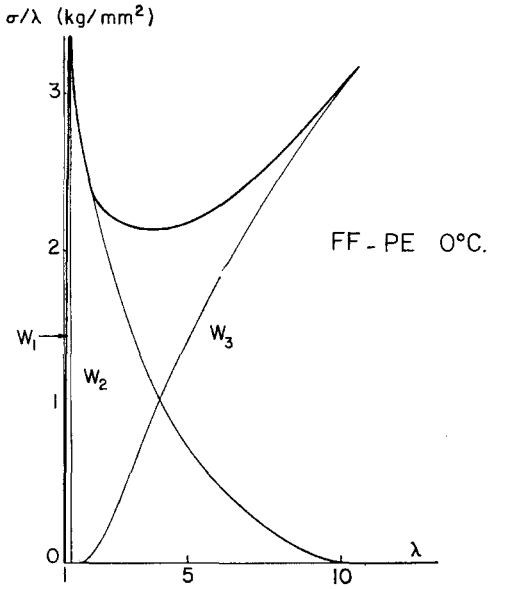

Figure 7 The differential work density $\sigma/\lambda = \sigma_n$ and the separation of contributions to W_2 and W_3 as functions of draw ratio λ for quenched linear PE drawn at 0°C.

polymers. The mechanical properties of the volume element definitely indicate the existence of the three fundamental stages of the plastic deformation. Their connection with crystal organisation can be based on the morphological evidence obtained from X-ray data and electron microscopy. But a detailed model of plastic deformation which would consider the role of crystals, amorphous component, and intercrystalline molecular links cannot be derived from such mechanical data alone as discussed in this section.

3. X-ray Scattering

Wide-angle X-ray scattering (WAXS) provides exact information about crystal lattice orientation from the spatial distribution of diffraction maxima, and about crystallite size and lattice disorder of first (thermal vibration) and second (paracrystalline disorder) order from the radial width of the maxima. From such data, can be derived the random orientation of lamellae in the original microspherulitic sample, the orientational changes during the morphology transformation, and the more or less perfect orientation of crystallised polymer chains in the fibre structure generated in the neck. In the neck itself a gradual transition from the former into the latter morphology is observed. The extension of coherently scattering crystaline lattice in the chain direction (D) turns out to be a bit smaller than the lamella thickness L derived from small-angle X-ray scattering (SAXS), in excellent agreement with the polymer crystal model assuming a crystalline core and a noncrystalline or "amorphous" surface layer [2]. Some recent investigations of PE single crystals [24-26] indicate that the lateral extension of lattice coherence is also proportional to L. These results apply equally, with some differences in numerical values, to the microspherulitic and fibre structure. It may be concluded from this data that the mosaic structure of polymer crystals is as well established as that of crystals of low molecular weight material. The ratio of about 2:3 between the extension of the mosaic block in the chain direction and the extension in the direction perpendicular to it invites the speculation about the same ratio of free energy requirements of the corresponding surfaces. With $\sigma_3 \sim$ 60-80 erg/cm³ for the lamella surface with folds, $\sigma_1 = \sigma_2 \sim$ 90-120 erg/cm² is obtained for the interfaces between the blocks [25]. Hence, a high defect concentration or a supercooled "liquid" (liquid crystal) layer seems to be sandwiched between adjacent mosaic blocks.

The study of crystallographic disorder yields a higher degree of paracrystalline disorder and, hence, a lower density of the crystalline component of the fibre structure obtained by drawing at low temperature, e.g. below 110°C for PE, as compared with that of the unoriented, microspherulitic material slowly cooled from melt or subsequently annealed. The density very nearly corresponds to that of quenched PE [21, 27]. The differences of the crystallographic disorder between the fibre and the microspherulitic section of the same sample disappear completely if the drawing is performed at a high temperature, i.e. above 110°C.

Very little information about the amorphous component can be obtained from WAXS. An increase in the radius of the amorphous ring in drawn PE was interpreted as a reduction of lateral chain-to-chain distance, and, hence, as an increase of density of the amorphous component [28].

SAXS yields information about lamella packing, orientation, and long period. The random orientation of stacks of lamellae of the microspherulitic structure is replaced by extremely well oriented lamellae of the fibre structure, either perpendicular (two-point diagram) or at

an angle (four-point diagram) to the fibre axis. The surface of lamellae may vary in orientation within rather large limits as can be deduced from the lateral width of the meridional maxima. The combination of intensity of SAXS (Porod's invariant [29]) with density of the bulk and the amorphous component yields information about true crystallinity and the reduced density of the crystalline component [28] in good agreement with the information on the increased para-crystalline disorder obtained from WAXS. The analysis of radial width [30] of SAXS maxima can be used for the determination of the thickness of amorphous (l) and crystalline (D) layer of the sandwich type stacked lamellae with a period $L = D + l$.

But the most surprising and new information yielded by SAXS of PE and PP is the discontinuous change of long period during drawing [31-39]. The effect is particularly conspicuous with drawing at low temperature if the initial L of the microspherulitic structure is larger than that of the new fibre structure. The new period appears with the first SAXS pattern (meridional maximum) attributable to the fibre structure [39] and remains constant very nearly independently of the draw ratio. There is a small dependence on the draw rate; the long period decreases slightly with increasing $\dot{\epsilon}$. The main dependence is on the temperature of drawing (fig. 8). From SAXS and WAXS it can be deduced that the transformation from the microspherulite into fibre structure occurs in a finite range of draw ratio (see fig. 1 in [35]). Therefore, the discontinuous change in long period occurs over a finite volume of the sample.

The surprising fact is that the long period of the starting material does not play any detectable role in determining the new long period. This is the first indication that the deformation process in the neck which transforms the microspherulitic morphology into the fibre structure must be a very drastic elementary process, discontinuously changing the folded chain arrangement in the crystalline blocks. A simple rotation of lamellae from the random orientation to the more or less perpendicular orientation to the draw direction simply would not yield such a change of long period, but would instead demand a long period closely correlated with that of the starting material in striking contradiction to experimental data.

A change in long period demands a substantial mass transport inside every crystal. The

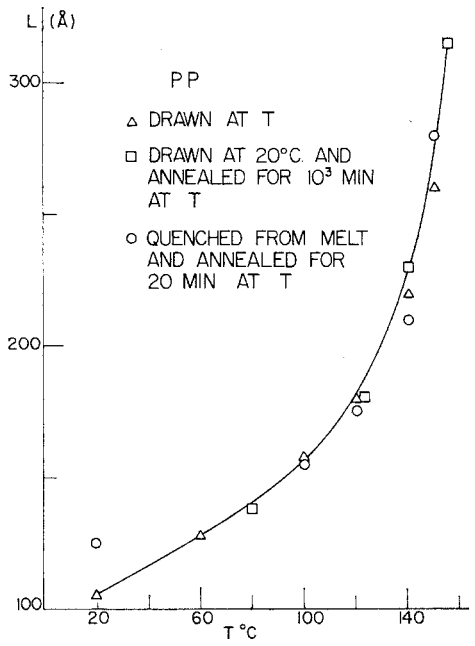

Figure 8 Long period L of drawn isotactic PP as function of temperature T of drawing (△), drawn at 20° C and annealed for 10^3 min at T (□), quenched from melt and annealed for 20 min at T (○) (Baltá-Calleja and Peterlin [39]).

case was thoroughly investigated in connection with long period growth during annealing [40, 41]. The mass transport mainly occurs by longitudinal sliding motion of chains in the crystal lattice. In the vicinity of the melting point, i.e. above 110°C in the case of linear PE, this type of mobility indeed becomes sufficiently large for a substantial increase of long period during annealing. Note, however, that annealing never leads to a decrease of long period. The deformation work in the neck (W_2) expended for the transformation from the microspherulite into fibre structure is indeed sufficient for quite a substantial local rise of temperature if no heat dissipation occurs to the environment (adiabatic drawing). In such a case with linear PE the maximum possible temperature values between 40 and 110°C are obtained if drawing is performed between 0 and 90°C (fig. 9) [21]. This is definitely not enough for a substantial chain mobilisation except at the highest temperature of drawing.

From the data in fig. 3 one sees that the transformation from spherulitic to fibre structure is not yet completed in the newly formed neck ($d = 0$). The substantial deformation occurring

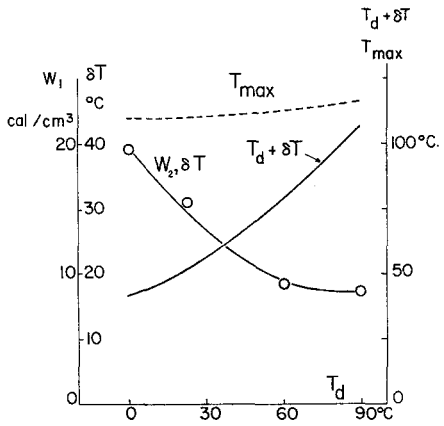

Figure 9 Temperature rise δT and the temperature attained $T + \delta T$ of the volume element where the neck started as a consequence of the adiabatic heating effects of the deformational work W_2 for morphology transformation (full lines) and the maximum temperature (T_{max}) reached (broken line) if the whole plastic deformational work $W_2 + W_3$ is considered for heating.

after the neck certainly includes a large amount of such transformation. In the extreme case it can be assumed that the whole work density $W_2 + W_3$ of deformational forces is needed for the transformation and is, therefore, heating the volume element. With this upper limit of transformational work density, substantially higher heating effects are obtained (broken line in fig. 9). The maximum temperatures reached (110 to 120°C) are very nearly independent of the temperature of drawing. They are well within the range where large modifications of long period occur during annealing and are close enough to the melting temperature so that partial melting becomes possible but not enough heat is produced for complete melting. Moreover, it is certain that not the whole work $W_2 + W_3$ is spent on lamella destruction and the concurrent chain unfolding. The actual transformation work and, therefore, the heating effect will be somewhere between the two limits given by W_2 and $W_2 + W_3$ and so will be the temperature reached in the destruction zone between $T + \delta T$ and T_{max} of fig. 9. Hence, very likely little or no true melting may take place. But it is strange that, in contrast with the long period growth during annealing an adjustment of the long period obtains in the drawing experiment, i.e. either an increase or a decrease, depending on the starting value L_0, to a value which is a unique function of the temperature of drawing. This function is very similar to, and slightly above, that obtained by isothermal crystallisation and nearly identical with the values obtained after prolonged annealing of drawn and undrawn samples (fig. 8).

Another possibility is a high chain mobilisation by a process similar to partial melting or transition into a liquid crystal phase even at a temperature below the melting point (130°C). Such a phase transition may be eventually brought about by the high tension stresses and the large reduction of the cross-section in the bundle of microfibrils produced in the micronecking zone which to some extent may act as a very high negative pressure. A melting point depression of about 70°C per kilobar negative pressure can be expected from the extrapolation of the melting data in the pressure range between 1 bar and 1 kilobar [41a]. Such a "pseudomelt" or liquid crystal without any substantial chain randomisation would yield, during the subsequent cooling to the ambient temperature, a long period corresponding to the temperature at which the "pseudomelted" chains would reorder into a normal crystal lattice. If such a "crystallisation" occurs after cooling to the temperature of drawing, then indeed, a long period not much different from that obtained by isothermal crystallisation at the same temperature can be expected. This model seems to be supported by data on linear and branched PE [34] where the long period could be described by $L_T = A + B/(T_m - T_d)$ up to a supercooling of 100°C. Here T_m is the melting temperature of PE drawn at room temperature to a draw ratio of 6 and A, B are constants depending on branching. At larger relative supercooling, i.e. for $T_d < T_m - 100°$, the long period remains constant $L_T = A + B/100°$. This means that at the rate of drawing of the experiment the mobilised chains can be supercooled up to a maximum of 100°.

Not much is known about polymer "crystallisation" from such a highly mobilised and aligned pseudomelt or liquid crystal. But the small change in conformational entropy would certainly favour a larger L than that obtained in crystallisation at the same temperature from a completely randomised melt. Another problem is how to explain the much larger supercooling up to 100°C in contrast with $\Delta T < 40$°C for crystallisation from unoriented PE melt before the reorganisation into the normal orthorhombic crystal lattice takes place.

Whichever mechanism is considered many

unsolved problems still remain which defy proper formulation. But the experimental facts demand a sufficiently high chain mobility for explanation of the long period change which may be quite drastic if a sample with high L_0 is drawn at a low temperature yielding a small L_T. Neither the work density W_2 nor $W_2 + W_3$ is sufficient for raising the temperature to the melting point and supplying the heat of fusion, so that normal melting with perfect chain randomisation can be excluded as an explanation for the effect.

4. Electron Microscopy

While the X-ray diffraction evidence for the deformation process is rather indirect as far as morphology is concerned, electron microscopy yields direct observation of single steps involved. With increasing strain the plastic deformation of PE single crystals [1, 44, 45] shows phase transformation and twinning, chain slip and tilt, and finally the formation of cracks bridged by a great many microfibrils if the crack cuts through the chain folds and the molecular weight is large enough. The microfibrils originate at the crack edges at micronecks which transform the lamellae into the fully oriented fibre structure (fig. 10). Wide-angle electron scattering shows the perfect alignment of crystallised chains in the microfibril axis; dark field electron microscopy shows discrete crystal blocks as parts of every microfibril [42, 43]; iodine staining shows a regular alternation in the fibre axis of more and less iodine permeable sections [47]. These observations are compatible with a microfibrillar model consisting of small fully oriented crystal blocks alternating with amorphous regions. The lateral dimensions of the blocks of the microfibril are of the same order of magnitude as the lateral dimensions of the mosaic blocks of PE single crystals [24]. The longitudinal dimensions of the blocks are close to those of the original lamellae, thus yielding a close correlation between block and lamella thickness [48].

Figure 10 Microfibrils pulled out at the crack of POM single crystals (Ingram [46]).

The mechanism of crystal fracture into single blocks of folded chains partially unfolds the molecules connecting two adjacent blocks and incorporates the unfolded sections as tie molecules into the microfibril [3]. Since every microneck transforms a section of the single crystal significantly wider than the width of the microfibril, the blocks from different parts of the section feeding the same microneck are most likely not incorporated into the microfibril in exactly the same order as they were arranged in the lamella. Therefore, the unfolded chains connect as tie molecules not subsequent blocks, but more often blocks a little farther apart. Such a situation significantly increases the fraction of tie molecules passing through the amorphous layer sandwiched between two subsequent blocks and, hence, the longitudinal strength of the microfibril.

Since all microfibrils at a crack of a single crystal have a very similar cross-section A_{mf}, each of them contains in first approximation the same amount of fibrous material pulled out of the single crystal of thickness L. If n microfibrils per unit length of the crack pertain and a depth a is transformed into microfibrils of length b (fig. 11), then from conservation of volume it follows that

$$nA_{mf}b = aL$$

and from that the draw ratio

$$\lambda_{mf} = b/a = L/nA_{mf}$$

inversely proportional to the density of microfibrils. Since a low molecular weight sample does not yield any microfibrils at the crack and the chances for long range connections by a single molecule increase with increasing M, it can safely be concluded that the number of microfibrils will show a tendency to increase with molecular wieght. Consequently, the draw ratio

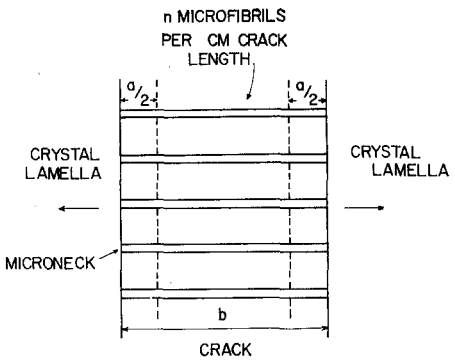

Figure 11 Draw ratio $\lambda_{mf} = b/a$ of microfibrils pulled out at the single crystal crack. A depth $a/2$ of the lamella at each side of the crack was transformed into microfibrils of length b.

λ_{mf} will decrease with M. The effect will depend more on M_w than on M_n because the deciding factor is the volume fraction occupied by the molecules and not their number. The increase of n with M also means a smaller section $1/n$ of the crystal feeding one microneck and, hence, a shorter distance in the microfibril between a pair of initially adjacent blocks connected by the unfolded sections of molecules bridging their original boundary. This means an effective reduction of tie molecules and, therefore, a reduced tensile strength. The effect may be partially compensated in high molecular weight samples by the greater number of molecules bridging the boundary between adjacent blocks of the original lamella.

One still assumes in some places that the microfibrils contain fully extended chains obtained by chain unfolding in the microneck (see for instance fig. VIII-57 in [1]). The draw ratio in such a case turns out to be $\lambda_{mf} = L/d$ where $d = 4.1$Å is the distance between adjacent straight sections of the same PE macromolecule in the crystal if (1 1 0) is the growth plane. With $L = 200$Å one has $\lambda \sim 50$ which is much more than one ever obtained in drawing of bulk PE. Moreover, in the case of complete chain unfolding the draw ratio would be directly proportional to the long period L, i.e. large for annealed ($L \sim 400$Å) and small with quenched ($L \sim 160$Å) samples in contradiction with experimental data [21] which show a very small difference between the two cases.

The microfibrils show a tendency for lateral coalescence which decreases the surface-to-volume ratio. The effect is particularly conspicuous in the case of multilayer crystals and extremely thin membranes (two-dimensional spherulites) which produce such a great number of microfibrils that one obtains a two-dimensional fibre structure which is ideally suited for electron diffraction and dark field electron microscopy studies (fig. 12) [42, 43]. Such thin layers are, indeed, ideal model systems bridging the gap between single crystals and bulk samples. Very nearly the same mechanism of transformation from the lamellae of the spherulitic sample into the fibre structure operates in the deformation of all the cases. The discontinuous step is the transformation of every lamella into microfibrils by micronecks.

Surface replicas of the neck area show the random distribution of crystal cracks bridged by a nearly continuous agglomeration of microfibrils [42, 49]. The microfibrils are easily observed in the drawn material after some lateral tension or a shearing stress was applied [1]. The lateral coalescence with preferential contacts between adjacent crystal blocks yields lamellae more or less perpendicular to the draw direction, which are observable after etching away of the amorphous component (ion bombardment, fumic nitric acid treatment) [50]. The long period observed by electron microscopy of surface replicas agrees very well with the values derived from SAXS thus supporting the view that the electron microscopy and SAXS describe the same morphology.

It is quite important to stress again that the lamellae of the fibre structure are not the primary element of the morphology. The basic element is the folded chain crystal blocks which are incorporated into microfibrils and held together in the axial direction by a great many tie molecules. The microfibril is, therefore, the strong unit which determines the elastic modulus and the tensile strength of the fibre structure. There are very few, if any macromolecules connecting adjacent blocks of different microfibrils forming the same lamella. The relatively good lateral fit of the crystal blocks yields the lamellae which are oriented more or less perpendicularly to the fibre direction. The flow field in the neck may eventually favour a skewed orientation [51], particularly in rolled samples [52, 53] and in drawn high molecular weight material [20].

But there are two important features in bulk samples with no counterpart in single crystal drawing: the change of long period and the creation of interfibrillar tie molecules. The blocks

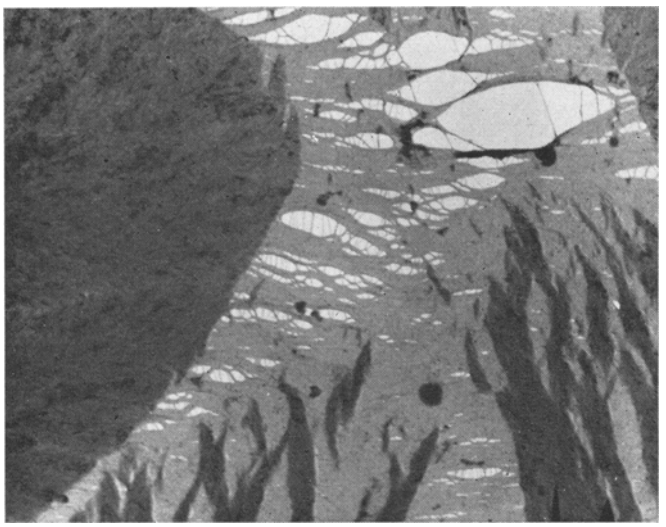

Figure 12 Electron micrograph of deformed ultrathin PE film showing the mainly coalesced microfibrils and the remains of incompletely transformed spherulitic structure (Sakaoku and Peterlin [42]).

in microfibrils pulled out of single crystals show a straightforward connection with the mosaic blocks of the original lamellae so far as thickness is concerned. In bulk samples, however, a striking change of long period occurs which obliterates any connection with the long period of the starting material. The explanation of this difference must lie in the different geometry of both cases because all other material properties are very nearly the same.

Peterlin and Sakaoku [54] suggested the following model for the destruction of lamellae in the bulk sample which, indeed, takes into account such an effect. The parallel packing of lamellae into stacks of a few thousand angstroms thickness remains very nearly unchanged during the first preparatory stage of plastic deformation before the neck. After chain tilt and slip, and lamella rotation, the whole stack assumes a position most favourable for lamella destruction by micronecking. As a consequence of stress concentration a planar arrangement of micronecks is established in a thin destruction zone passing through the whole stack. The nearly identical drawing conditions in the zone yield parallel microfibrils of practically the same draw ratio which, as a rule, differs from that of the adjacent regions. The existence of such fibrillar regions having different draw ratios can be detected by electron microscopy of annealed samples [50, 54].

The geometry of the destruction zone, which is a few hundred angstroms thick and a few thousand angstroms wide, imposes a specific flow pattern of the heat generated by lamella destruction in the micronecks. In an area behind the zone – nearly as long as the zone is wide – there is practically no chance for heat transfer to the environment. As a consequence the fibrous material generated in the destruction zone remains for a long period of time at the theoretically maximum temperature caused by the conversion of destruction work into heat. In contrast with this adiabatic effect in bulk sample drawing, the point or line source type of arrangement of micronecks in the drawing of single crystals immediately leads to a substantial heat transfer to the environment, so that the temperature never reaches the theoretically possible value. The drawing is nearly isothermal. The smaller heating effect (insufficient for significant chain mobilisation) leaves the folded chain blocks unchanged, in contrast with the situation in bulk samples where the heating produces a temperature sufficient for so much chain mobilisation that during subsequent cooling to ambient temperature a long period can be established corresponding to this temperature. This explanation does not explain the actual type of chain mobilisation, whether it is of the same type as observed during long period growth, a partial melting with very little if any chain randomis-

ation, or a liquid crystal formation (smectic or nematic phase).

Since the high adiabatic local heating effect is confined to extremely small areas with average dimensions between 1,000 and 10 000Å widely separated from each other and randomly scattered in the neck, the heat shows up in a temperature increase of the neck in exactly the manner as calculated by Vincent [14], who considered the sample as a continuum. The molecular model shows that the actual heat generation in a crystalline polymer in the neck is not continuous but confined to discrete destruction zones.

Another effect concerns the interfibrillar tie molecules originating from tie molecules connecting the lamellae of the original sample. Such connections occur during crystallisation from melt if separate parts of the same macromolecule are included in the crystal lattice of different lamellae (fig. 1). The intervening section is prevented from achieving complete crystallisation and remains as a tie molecule in the amorphous layer between the crystals. The number of such ties increases with the rate of crystallisation and the weight average molecular weight M_w. It is larger in quenched than in slowly cooled, or annealed samples. The tie molecules increase the toughness and to some extent the susceptibility of the sample to plastic deformation. On the other hand, they connect microfibrils originating from the two connected lamellae and as interfibrillar tie molecules impose a limitation on the draw ratio of the microfibrils and, therefore, on that of the bulk sample. This limitation can be quite severe with very high molecular weight samples (ACX with $M_w = 1.5 \times 10^6$) where the large number of tie molecules in the undrawn material yields a very low crystallinity [20]. The maximum draw ratio (natural draw ratio) in this case is only about 4. Such a decrease of λ_∞ although less drastic was already observed by Williamson *et al* [19]. in medium molecular weight linear PE.

The interfibrillar tie molecules exert strong torsional moments on the folded chain blocks to which they are attached and, hence, tend to produce or accentuate a finite inclination of the lamellae to the draw direction which may have been already caused by a shearing flow component in the neck [54]. The most conspicuous effect of interfibrillar tie molecules is manifest in the lamella rotation [10, 50, 55, 56] and shrinkage [34] during annealing. The "noncrystalline" interfibrillar tie molecules in the boundary layers between adjacent microfibrils become sufficiently mobilised at relatively low annealing temperatures to exert a strong entropic contractive force between the ends anchored in crystal blocks of two different microfibrils. The generation of such tie molecules during micronecking produces a strong, unidirectional orientation so that there results a finite force and torque of all tie molecules between two adjacent microfibrils. This torque produces the rotation of lamellae during annealing and, hence, disorients the sample. The longitudinal forces tend to slide the microfibrils past each other in the direction opposite to that during the drawing process, and they can indeed do so as soon as the annealing temperature reduces sufficiently the frictional resistance to such a sliding motion. According to this mechanism, the shrinkage occurs at a lower temperature than the long period growth, which demands sufficient mobility of chains in the crystal lattice.

A substantial contribution to shrinkage comes also from intrafibrillar tie molecules connecting two blocks which are not immediately following each other. Such tie molecules tend to bring together again the crystalline blocks separated during micronecking. By this process the microfibrils become shorter and thicker, a process very generally observed on annealed isolated microfibrils (fig. 1 in [47]). Concurrently, a substantial disorientation is also produced which involves a rotation of crystal blocks without any – or with very little – sliding chain motion in the crystals (fig. 3b in [56]).

As a rule annealing partially reverses the last steps of plastic deformation [49]. In the extreme case of total melting, but not yet complete randomisation, the drawn sample may be even returned very nearly to the original shape and structure [57]. The driving force for such a reversal is the strained tie molecule which tends to assume more probable random conformations. The relaxation resulting from contraction of tie molecules during shrinkage also leads to inclusion of substantial sections of the initially noncrystalline ties into the crystalline lattice, thus increasing the crystallinity. If the sample is clamped at the ends and, therefore, not free to shrink, the microfibrils are rather well fixed. In such a case the relaxation of interfibrillar tie molecules mobilised during annealing may occur by partial pulling through the crystal lattice and inclusion of properly located sections into the crystal lattice of the folded chain blocks. By such

a process no free tie molecule sections are left beyond those connecting subsequent blocks. These sections assume amorphous conformations as much as possible. The relaxation of intrafibrillar tie molecules occurs by pulling some chain sections through the crystal blocks, thus making the tie molecules so much longer that they can assume a more amorphous conformation.

The role of intra- and interfibrillar tie molecules as just described is not so much derived from direct experimental evidence as from general physical principles and the geometry of the basic deformational modes. Electron microscopy is hardly capable of showing such molecules or elucidating their conformation, but two other techniques proved to be very helpful in this connection: infrared absorption and fumic nitric acid etching.

5. Infra-red Dichroism

By measurement of the absorption and polarisation of the crystalline band at 1894 cm^{-1}, and the amorphous bands at 1368, 1303 and 1078 cm^{-1}, information is obtained about the orientation of crystals and molecular chains in the amorphous component of drawn PE [58, 59]. This information confirms that the orientation of the crystalline band proceeds very fast with increasing draw ratio in complete agreement with WAXS data on crystal orientation with drawing. The orientation of the amorphous chains, however, is much slower and never reaches the same high level of completeness as that of the crystals. Among the more or less regular chain loops, free chain ends (cilia), and tie molecules constituting the amorphous layer, only the tie molecules may be completely oriented by the drawing process as a consequence of the high tensile stress in the draw direction. Assuming complete orientation of tie molecules in a highly drawn sample, the fraction of tie molecules can be determined from the intensity of the IR band corresponding to sequences of *trans* conformation. The fraction proves to be about 25% at a draw ratio of 15 and proportionately less at smaller λ. Higher λ does not improve the orientation. Annealing again drastically reduces the orientation in the amorphous components long before a substantial disorientation of crystals becomes observable. Since in the sample investigated (Lupulene with 7 nonterminal CH_3 groups per 10^3CH_2, $M_n = 12\,000$, $M_w = 80\,000$) about 39% of the amorphous material is expected to be cilia, the contribution of the loops proves to be about 36% at $\lambda = 15$. No other method yields such a detailed analysis or estimate of the amorphous layers and their dependence on thermal and mechanical history of the sample.

6. Fumic Nitric Acid Etching

The acid etching method [60] proved to be extremely useful in the preparation of bulk samples for surface replica electron microscopy by exposing the crystal core of stacked lamellae so that by metal shadowing the interlamella boundaries can be made observable. Fuming nitric acid attacks the amorphous much faster than the crystalline regions of PE, so that after a while the samples contain merely the crystal core of the lamellae stripped from the loops and cilia of the "amorphous" surface layer. The investigation of weight loss and molecular weight of etched samples, indeed, shows a rapid progress of etching and a drastic drop in molecular weight in the first stage when the amorphous component is destroyed. The etching and molecular weight decrease are slower in the second stage during which the crystal core is attacked primarily from the (001) planes, i.e. in the direction of chains ends. The inflection in the weight loss or molecular weight curves, occurring at about 20 h of etching at 80° C, yields a value for the amorphous component, crystal core, and lamella thickness in good agreement with density and SAXS data [61].

A systematic study of drawn PE revealed some interesting new facts in connection with tie molecules [22, 62]. The experimental procedure was as follows: The sample was etched for about 170 h (one week), thoroughly washed, dried, and then run in a differential scanning calorimeter (DSC). The first run was quite conventional with a single melting peak. If the melt was solidified by slow cooling and then run again in the DSC, a completely different melting curve with two maxima was observed. The conclusion is that in the etched sample two molecular weight species were present, but so intimately mixed that they yielded a composite material with a single melting point. The crystallisation of the once melted material, however, achieves a complete separation of the components and yields two types of crystals with two distinct melting curves which partially superimpose in the second run thermogram. With the known relationship between melting temperature and crystal thickness obtained from data on etched single crystals, the length of

the molecules corresponding to the two melting peaks can be determined. Since the etching time was long enough to remove all of the chain section in normal amorphous conformation, a safe conclusion is that the high molecular component of the debris represents tie molecules connecting subsequent lamellae. They are in highly stretched conformation and, therefore, resistant to acid attack. The fraction of tie molecules calculated from the melting curves increases nearly linearly with the draw ratio up to $\lambda = 15$ and then levels off at $\lambda \sim 20$. For low draw ratios up to $\lambda = 8$ their number seems to be independent of the temperature of drawing [22]. At higher λ their number increases quickly with decreasing temperature of drawing [63]. The elastic modulus and stress to break, measured at $-180°C$ in order to prevent large scale plastic deformation before fracture of such samples, vary in almost the same manner with draw ratio and temperature of drawing as the number of tie molecules.

The tie molecules of drawn PE are highly strained and aligned, therefore having denser packing and substantially fewer gauche conformations. This results in a higher density [28, 64] and smaller heat content [65, 66] of the amorphous component compared with perfectly relaxed supercooled liquid. Both effects disappear with heating, i.e. if the drawing is performed at higher temperature or during annealing (above 100°C in the case of linear PE). Particularly conspicuous are the changes in sorption, diffusion and permeability of gases and vapours resulting from the nonequilibrium conditions of the amorphous component [67]. In PE drawn to a draw ratio of 15 at 60°C, the sorption of methylene chloride is reduced to about 17%, the diffusion constant to 0.5%, and the permeability to 0.1%. The sorption is independent of temperature as in undrawn samples, indicating that the energy conditions of the sorption sites remain unchanged by drawing, merely their number being reduced. The activation energy for diffusion, however, increases by nearly 100%. This may be interpreted either to be a higher energy requirement for formation of a hole for the diffusant molecule in the denser amorphous component, or to be the need for formation of a longer tunnel between two available sorption sites which are situated farther apart in the drawn than in the undrawn sample. These drastic effects are observable only at rather high draw ratios ($\lambda \geqslant 9$) and low temperature of drawing ($T_d < 100°C$), i.e. where, indeed, the whole sample is transformed into the fibre structure and no relaxation has taken place in the amorphous component. At lower λ the effects are disproportionately smaller as a consequence of the finite content of undrawn material [68].

7. Molecular Model of Plastic Deformation

In the foregoing description of experimental data connected with the transformation of the microspherulitic, macroscopically isotropic initial material into the highly oriented fibre structure, the molecular model was presented as it gradually formed under the challenge of accumulated evidence. It seems now proper to recapitulate its main features and formulate them in a manner which best corresponds to the presently known facts.

The plastic deformation of PE and PP proceeds in three steps:

1. *The continuous plastic deformation of the spherulitic structure before the neck* involving shear, slip, and rotation of stacked lamellae, phase transformation and twinning, chain tilt and slip inside every single lamella. By such effects the material is softened and prepared for the next discontinuous step which transforms the spherulitic into fibre structure. However, during this whole first stage the individuality of spherulites, stacks of lamellae, and of single lamella remains preserved. The main effect of this first stage is the rotation of the stacks of parallel lamellae into a position where, as a consequence of the concurrently attained chain tilt, the plastic compliance is maximum for lamella destruction by longitudinal chain slip. Such a slip occurs primarily in the boundary layer between adjacent crystal blocks which contains such a high concentration of crystal defects that it is nearly amorphous.

2. *The discontinuous transformation in the neck from the spherulitic to the fibre structure.* It proceeds by transformation of every lamella by micronecks into a bundle of microfibrils, the basic element of the fibre structure. Blocks of folded chains are broken off the lamellae by longitudinal chain slip in the "noncrystalline" boundary layers between adjacent blocks and incorporated in the microfibril. Because the microfibrils at the single crystal crack are spatially separated from each other, each microneck has to transform a section of lamella wider than the microfibril. Hence, the folded chain blocks are

not incorporated in the microfibril in exactly the same order as they were arranged in the lamella. Therefore, the tie molecules, as a rule, do not connect immediately adjacent blocks but rather blocks farther apart, thus crossig all the intervening amorphous layers. The ensuing increase in the number of tie molecules per amorphous layer sandwiched between subsequent crystals, is proportional to the reciprocal number of microfibrils per unit length of the crack and, hence, to the draw ratio of the microfibril. The draw ratio decreases with the molecular weight of the sample. Moreover, the fact that, as a rule, intrafibrillar tie molecules are connecting blocks farther apart provides a mechanism for shrinkage and block disorientation during annealing. The tendency of the tie molecules to contract reverses to some extent the deformational process.

The whole stack of parallel lamellae subjected to the same stress field, rotation, chain slip, and tilt during the first stage of plastic deformation simultaneously attains the optimum state for micronecking. As a result of stress concentration the micronecks will be arranged in a thin zone crossing the whole stack. Such a concentration of micronecks yields almost the same draw ratio for all the microfibrils produced, and a tendency for lateral fit of crystalline blocks leading to the formation of lamellae more or less perpendicular to the draw direction and extending over the whole cross-section of the fibril. Every fibril differs from adjacent fibrils mainly in the draw ratio λ. As a consequence of this difference, a poor auto-adhesion exists on the boundary between such fibrils. It leads to extended longitudinal voids and favours the longitudinal slip of fibrils which results in the fibrillation tendency of highly drawn PE and PP.

Interlamella tie molecules of the original sample connect, after the transformation in the necking zone, blocks of different microfibrils. Their number increases with molecular weight and the rate of crystallisation of the starting material. Such interfibrillar tie molecules may add to the lateral cohesion of the fibrils, but also interfere with the longitudinal sliding motion of the microfibrils during micronecking and the additional plastic elongation of the fibre structure. Their arrangement seems to be unidirectional so that they exert a finite tensile force and torque on the crystal blocks they connect. A manifestation of such forces generated by the flow pattern during deformation and drawing of microfibrils is the skewness of lamella orientation in the fibre structure. But their main effects are the retractive force leading to fibre shrinkage by back sliding of microfibrils and the torque producing crystal disorientation during annealing with free ends.

In the drawing of bulk samples, independently of the long period of the initial material, a long period of the fibre structure is established which depends on the temperature of drawing in very nearly the same manner as the long period of unstrained bulk samples depends on the temperature of crystallisation. A high chain mobilisation is needed for such an adjustment. The deformation work in the destruction of lamellae substantially raises the temperature, but does not produce enough heat for complete melting even if there is no heat dissipation to the environment. Therefore, it seems probable that the high temperature and the negative pressure tensile stress and lateral contraction produce a "pseudomelt" with very little if any chain randomisation, i.e. a liquid crystal. It must remain fluid during cooling behind the necking zone and must not crystallise before the temperature reaches that of the environment (temperature of drawing). This temperature determines the long period of the reformed crystals. In the case of branched and linear PE such supercooling may reach 100°C.

The difference in geometry – a linear arrangement of isolated micronecks in a single crystal, on one hand, and the two-dimensional arrangement in the destruction zone of a stack of lamellae in bulk samples, on the other hand – yields the maximum possible temperature rise in the latter and a much smaller rise in the former case. Such a difference in the maximum temperature, and hence in the chain mobilisation attained in the micronecks, would be a reasonable explanation of the striking difference between the long period modification in bulk material and its constancy in single crystals. On the other hand, the temperature rise in, and immediately behind the more or less randomly distributed destruction zones, i.e. in cubic areas with an edge length close to the lateral dimensions of the ones, does not interfere with the normal heat dissipation and the observed temperature rise in the neck. Because the zones are only a few thousand angstroms wide no macroscopic temperature increase beyond that calculated from conventional heat dissipation in the neck can be observed.

3. *Plastic deformation of the fibre structure after*

the neck. Such a deformation can occur only by sliding motion of the microfibrils or fibrils past each other, thus stretching the interfibrillar tie molecules and unfolding the chain sections by which the tie molecules are anchored in the crystal blocks of adjacent microfibrils. As may be deduced from fig. 3 this type of deformation is quite substantial for the volume elements where the macroscopic neck started. The rapid increase in the length and alignment of the interfibrillar tie molecules during this process favours inclusion of properly located chain sections of such molecules into the crystal lattice of the adjacent blocks. Such a process increases the density, i.e. the crystallinity of the drawn material, but also the resistance to further drawing. The strain hardening proceeds up to the final break.

The last two steps of plastic deformation seem not to be completely separated. The initial neck yields a relatively small draw ratio. If it, indeed, transforms the spherulite structure completely into fibre structure this small draw ratio is the draw ratio of the micronecking process. The necked volume element, i.e. the new fibre structure, continues to draw at a smaller rate up to the final break.

With progressive drawing time the neck becomes sharper and the deformation in the neck gradually increases to the maximum possible value, i.e. to the natural draw ratio, so that no substantial extension of the fibre structure occurs after the neck and before the break. This means that the last two steps of plastic deformation are combined in the more mature neck established after the sample is drawn for a while. Such a situation occurs in large scale fibre drawing and is of great technical interest. According to this model the natural draw ratio is larger than the draw ratio of the micronecking process.

But it is possible that at low draw ratio, i.e. in the early stages of the necking process, the transformation into the fibre structure is not yet complete. The transformation of remains of spherulitic structure into fibre structure (fig. 12), i.e. the completion of unfinished micronecking, may produce quite a significant increase in draw ratio and hence bring the volume elements, deformed first, to the same draw ratio as is obtained in one step in the final neck. If this is the correct explanation of drawing, then the natural draw ratio is the draw ratio of the micronecking process. In the steady-state neck, all the microspherulitic material is transformed in the microfibrils. No significant deformation of the new fibre structure occurs after the neck is formed up to the final break. In such a case the longitudinal sliding motion of the microfibrils or fibrils must be efficiently blocked by interfibrillar forces, i.e. by van der Waals forces between adjacent crystal blocks and adjacent amorphous regions, and by interfibrillar tie molecules.

The true situation is very likely somewhere between the two extremes, as can be deduced from recently performed experiments on sorption and diffusion of drawn PE [68]. For drawing at 60° C the transformation from spherulitic to fibre structure seems to be completed at a draw ratio 9, which is a little higher than that of the original neck, but markedly smaller than the natural draw ratio. This means that in the original neck the transformation is only partial and is completed by subsequent deformation of the already necked material, while in the more mature neck the transformation of morphology and the plastic deformation of the new fibre structure occur simultaneously.

The above description of the model corresponds to cold drawing with necking and also applies with slight reservations to hot drawing without a neck. The main morphological difference is the location of destruction zones which in cold drawing are concentrated in the neck, but which in hot drawing are more or less randomly distributed all over the sample. But the high temperature of hot drawing significantly affects the properties of the polymer solid before and during drawing. A long period increase, reduction in the number of tie molecules, healing of crystal defects, relaxation of amorphous component and increased mobility of molecular chains in the amorphous and crystalline regions are all observed. As a result during hot drawing the resistance to chain tilt and slip is drastically reduced; there is no yield point. The new fibre structure is much more free of crystal defect than with low temperature drawing. The enhanced regularity of lamella packing allows the appearance of the second order maximum of SAXS. The larger long period reduces the number of intrafibrillar tie molecules. The number of interfibrillar tie molecules is reduced by the decreased number of interlamella tie molecules of the starting material.

Acknowledgement

The author would like to thank the Camille and Henry Dreyfus Foundation for the generous support of this work and also Dr P. Ingram for

the permission to include his unpublished electron micrograph (fig. 10).

References

1. For older work, see P. H. GEIL, "Polymer Single Crystals", (Interscience Publ., J. Wiley & Sons, New York, 1963) pp. 421-490.
2. E. W. FISCHER and G. F. SCHMIDT, *Angew. Chem.* **74** (1962) 551.
3. A. PETERLIN, *J. Polymer Sci.* **C9** (1965) 61; **C15** (1967) 427; **C18** (1967) 123.
4. I. L. HAY and A. KELLER, *Kolloid-Z. & Z. Polymere* **204** (1965) 43.
5. R. S. STEIN, *Proc. R. A. Welch Foundation Conf. Chem. Res.* **10**: Polymers, (1967) 207.
6. R. BONART, *Kolloid-Z. & Z. Polymere* **211** (1966) 14.
7. A. PETERLIN, "Man-Made Fibers", Vol. 1, Ed. by H. F. Mark, S. M. Atlas, and E. Cernia, (Interscience Publ., J. Wiley & Sons, New York, 1967) pp. 283-340.
8. A. PETERLIN, *Kolloid-Z. & Z. Polymere* **216/217** (1967) 129.
9. A. PETERLIN, *Polymer Eng. Sci.* **9** (1969) 172.
10. E. W. FISCHER and M. GODDAR, *J. Polymer Sci.* **C16** (1969) 4405.
11. R. S. STEIN, *Polymer Eng. Sci.* **9** (1969) 320.
12. K. O'LEARY and P. H. GEIL, *J. Macromol. Sci.* **B1** (1967) 147; **B2** (1968) 261.
13. C. A. GARBER and P. H. GEIL, *Makromol. Chem.* **113** (1968) 251.
14. P. VINCENT, *Polymer* **1** (1960) 7.
15. A. KELLER and M. J. MACHIN, *J. Macromol. Sci.* **B1** (1967) 41.
16. K. KATAYAMA, T. AMANO, and K. NAKAMURA, *Kolloid-Z. & Z. Polymere* **226** (1968) 125.
17. H. D. KEITH and F. J. PADDEN, JR., *J. Polymer Sci.* **41** (1959) 525.
18. J. M. ANDREWS and I. M. WARD, *J. Mater. Sci.* **5** (1970) 411.
19. G. R. WILLIAMSON, B. WRIGHT, and R. N. HAWARD, *J. Appl. Chem.* **14** (1964) 131.
20. G. MEINEL and A. PETERLIN, *European Polymer J.*, in press.
21. G. MEINEL and A. PETERLIN, *J. Polymer Sci.* A2 **9** (1971) 67.
22. G. MEINEL, A. PETERLIN, and K. SAKAOKU, "*Analytical Calorimetry*," Ed. by R. S. Porter and J. F. Johnson, (Penum Press, New York, 1968) p. 15.
23. G. MEINEL and A. PETERLIN, *J. Polymer Sci.* **B5** (1967) 613.
24. R. HOSEMANN, H. ČAČKOVIČ, and W. WILKE, *Naturw.* **54** (1967) 278.
25. H. ČAČKOVIČ, R. HOSEMANN, and W. WILKE, *Kolloid-Z. & Z. Polymere* **234** (1969) 1000.
26. J. LOBODA-ČAČKOVIČ, R. HOSEMANN, and W. WILKE, *Kolloid-Z. & Z. Polymere* **235** (1969) 1162.
27. W. GLENZ and A. PETERLIN, *J. Polymer Sci.* **A2** in press.
28. E. W. FISCHER, H. GODDAR, and G. F. SCHMIDT, *J. Polymer Sci.* A2 **7** (1969) 37.
29. G. POROD, *Kolloid-Z.* **124** (1951) 83; *Adv. Polymer Sci.* **2** (1960) 363.
30. D. YA. TSVANKIN, *Vysokomol. Soed.* **6** (1964) 2078, 2083.
31. H. HENDUS, *Kolloid-Z.* **165** (1959) 32.
32. R. CORNELIUSSEN and A. PETERLIN, *Makromol. Chem.* **105** (1967) 192.
33. A. PETERLIN and R. CORNELIUSSEN, *J. Polymer Sci.* A2 **6** (1968) 1273.
34. A. PETERLIN and F. J. BALTÁ-CALLEJA, *Kolloid-Z. & Z. Polymere*, in press.
35. A. PETERLIN and G. MEINEL, *Makromol. Chem.*, in press.
36. R. T. SAMUELS, *J. Polymer Sci.* **C20** (1967) 253; A2 **6** (1968) 1101, 2021.
37. F. J. BALTÁ-CALLEJA and A. PETERLIN, *J. Mater. Sci.* **4** (1969) 722.
38. A. PETERLIN and F. J. BALTÁ-CALLEJA, *J. Appl. Phys.* **40** (1969) 4238.
39. F. J. BALTÁ-CALLEJA and A. PETERLIN, *J. Macromol. Sci.* **B4** (1970) 519.
40. A. PETERLIN, *J. Polymer Sci.* **B1** (1963) 279; *Polymer* **6** (1964) 25.
41. P. DREYFUS and A. KELLER, *J. Polymer Sci.* **B8** (1970) 253.

41a. S. MATSUOKA, *J. Polymer Sci.* **57** (1962) 569.

42. K. SAKAOKU and A. PETERLIN, *Makromol. Chem.* **108** (1967) 234.
43. K. SAKAOKU and A. PETERLIN, *J. Polymer Sci.* A2 **9** (1931) in press.
44. P. H. GEIL, *J. Polymer Sci.* **A2** (1964) 3813, 3835.
45. H. KIHO, A. PETERLIN, and P. H. GEIL, *J. Appl. Phys.* **35** (1964) 1599.
46. P. INGRAM, unpublished work.
47. A. PETERLIN, P. INGRAM, and H. KIHO, *Makromol. Chem.* **86** (1965) 294.
48. P. INGRAM, *Makromol. Chem.* **108** (1967) 281.
49. A. SIEGMAN and P. H. GEIL, *J. Macromol. Sci.* **B4** (1970) 557.
50. A. PETERLIN and K. SAKAOKU, "Clean Surfaces" Ed. by G. Goldfinger (M. Dekker, Inc., New York, 1970) p. 1.
51. N. KASAI and M. KAKUDO, *J. Polymer Sci.* **A2** (1964) 1955.
52. I. L. HAY and A. KELLER, *J. Mater. Sci.* **1** (1966) 41; **2** (1967) 538.
53. J. J. POINT, G. A. HOMES, D. GEZOVICH, and A. KELLER, *J. Mater. Sci.* **4** (1969) 908.
54. A. PETERLIN and K. SAKAOKU, *J. Appl. Phys.* **38** (1967) 4152.
55. K. SAKAOKU and A. PETERLIN, *Kolloid-Z. & Z. Polymere* **212** (1966) 51.
56. K. SAKAOKU and A. PETERLIN, *J. Macromol. Sci.* **B1** (1967) 103.
57. D. C. PREVORSEK and A. V. TOBOLSKY, *Text. Res. J.* **33** (1963) 795.
58. W. GLENZ and A. PETERLIN, *J. Macromol. Sci.* **B4** (1970) 473.

59. W. GLENZ and A. PETERLIN, *J. Polymer Sci.* **A2,** in press.
60. R. P. PALMER and A. T. COBBOLD, *Makromol.Chem.* **74** (1964) 174.
61. A. PETERLIN and G. MEINEL, *J. Polymer Sci.* **B3** (1966) 1059.
62. G. MEINEL and A. PETERLIN, *J. Polymer Sci.* **B5** (1967) 197, 613.
63. G. MEINEL, N. MOROSOFF, and A. PETERLIN, *J. Polymer Sci.* A2, **8** (1970) 1723.
64. W. GLENZ, N. MOROSOFF, and A. PETERLIN, *J. Polymer Sci.*, **B9** (1971) 211.
65. A. PETERLIN and G. MEINEL, *J. Polymer Sci.* **B3** (1965) 783; *J. Appl. Phys.* **36** (1965) 3028; *Appl. Polymer Symp.* **2** (1966) 85.
66. E. W. FISCHER and G. HINRICHSEN, *Koloid-Z. & Z. Polymere* **213** (1966) 28.
67. A. PETERLIN, J. L. WILLIAMS, and V. STANNETT, *J. Polymer Sci.* A2 **5** (1967) 957.
68. J. L. WILLIAMS and A. PETERLIN, *J. Polymer Sci.* A2, in press.

Received 23 November 1970 and accepted 10 March 1971.